Int. J. Non-Linear Mechanics, Vol. 27, No. 3, pp. 489 502, 1992
Printed in Great Britain.

0020-7462/92 $5.00 + .00
Pergamon Press Ltd

DYNAMICS OF SPINUP THROUGH RESONANCE

R. H. RAND

Department of Theoretical and Applied Mechanics, Cornell University, Ithaca, NY 14853, U.S.A.

R. J. KINSEY

Control Analysis Department, Aerospace Corporation, El Segundo, CA 90245, U.S.A.

and

D. L. MINGORI

Department of Mechanical, Aerospace and Nuclear Engineering, University of California at Los Angeles, Los Angeles, CA 90402, U.S.A.

(*Received* 4 *October* 1990)

Abstract—This work concerns the phenomenon of resonant capture, i.e. the failure of a rotating mechanical system to be spunup to a desired terminal state, due to its resonant interaction with another system or with itself. The phenomenon is important in the dynamics of dual-spin spacecraft. Starting from a simple mechanical system consisting of an unbalanced rotor attached to an elastic support and driven by a constant torque, we derive an abstract model of resonant capture. The model is investigated by using perturbation theory and elliptic functions. For a given system, the analysis predicts which initial conditions lead to capture. These predictions are shown to compare reasonably with the results of numerical integration.

INTRODUCTION

This work is motivated by a phenomenon observed in a dual-spin spacecraft (SC). A dual-spin SC consists of two bodies, a platform and a rotor, connected by a bearing assembly which allows relative rotation between the bodies, Fig. 1. When first placed in orbit, the platform and rotor rotate together with zero relative spin rate in an "all spun" configuration. Then a "despin maneuver" is initiated during which an internal motor provides a torque to increase the bearing axis component of the rotor angular velocity and decrease the bearing axis component of the platform angular velocity. Ideally, this continues until the platform is inertially non-rotating, at which point the motor is turned off. During despin, however, there are several ways in which the energy added to the SC by the motor may be channeled into motions other than the intended relative rotational motion between the platform and rotor. When this occurs, the state of the SC following despin ends up far from the desired state. One such failure during despin, referred to as precession phase lock (PPL), motivated this work. PPL is associated with a resonance in which the rotation of the rotor about the bearing axis becomes synchronized with the precession of the SC about its angular momentum vector [1].

In order to investigate this phenomenon, Yee [2] considered a simpler, but mathematically similar, system consisting of an unbalanced rotor attached to an elastic support and driven by a constant torque as in Fig. 2. He showed that, for a wide range of parameters, when the system was started from rest, the angular velocity of the rotor would increase until it reached the neighborhood of the natural frequency of the mass–spring system. Then, depending upon parameter values, the rotor's angular velocity would either continue to increase beyond the resonance region (a situation called *pass-through*), or it would remain close to the natural frequency of the mass–spring system (a situation called *capture*, see Fig. 3). In addition, even if the parameters are held fixed, a change in the initial conditions can affect whether a motion is captured or passes-through, see Fig. 3.

Sanders and Verhulst [3] also investigated this problem, and referred to the critical region of phase space in which the rotor angular velocity is close to the natural frequency of the mass–spring system as a *resonance manifold*. They showed that the time of passage through resonance depended on the initial conditions.

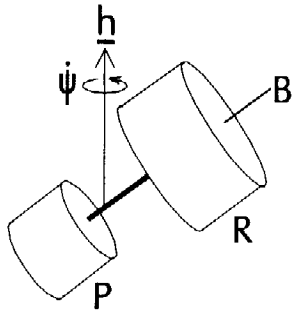

Fig. 1. Dual-spin spacecraft. P = platform, R = rotor, B = bearing axis, $\underline{h}$ = angular momentum vector, and $\dot{\psi}$ = precession rate.

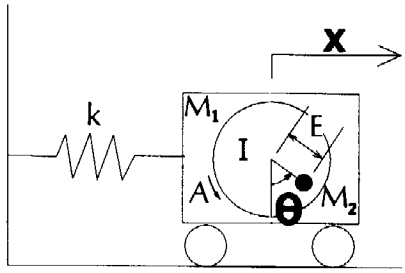

Fig. 2. A system consisting of an unbalanced rotor attached to an elastic support and driven by a constant torque [2]. See Appendix B, equations (B.1)–(B.10).

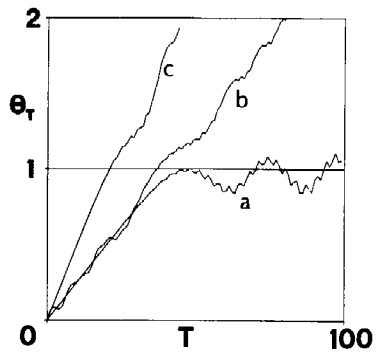

Fig. 3. Dynamics of the system of Fig. 2, equations (B.9) and (B.10) [2]. As the angular velocity $d\theta/dT$ approaches the (dimensionless) resonant frequency of unity, either the motion is "captured" (curve a) or it "passes through" the resonance (curves b and c). The question as to which of these outcomes occurs depends both on parameter values and initial conditions. All three curves correspond to $e = 0.1$, $\theta(0) = (d\theta/dT)|_{T=0} = (dz/dT)|_{T=0} = 0$. Curves a, b, c, respectively, correspond to the following values: ($z(0) = 0$, $L = 0.025$); ($z(0) = 0.4$, $L = 0.025$); and ($z(0) = 0$, $L = 0.05$).

In this paper we shall investigate a simple system which models the essentials of the capture vs pass-through dynamics. Our system can be derived from that of Yee [2] by a series of coordinate transformations which are presented in the Appendix. The derivation is approximate, and assumes that the unbalance and applied torque are small and that the rotor motion is close to resonance.

THE SYSTEM

We will investigate the dynamics of the system

$$\frac{d^2u}{dt^2} - u^2 = -w \tag{1}$$

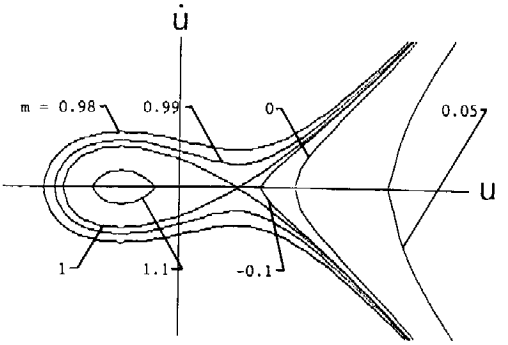

Fig. 4. Instantaneous phase portrait in the u–$\dot{u}$ phase plane for the system of equations (1) for $w = 1$. Each integral curve corresponds to a value of the squared modulus m of the elliptic function cn as in equation (4). Curves lying inside the separatrix loop correspond to $m \geq 1$ and are associated with capture. Curves lying to the left of the separatrix loop correspond to $m_2 < m < 1$, and are associated with pass-through. Region displayed is $-3 < u < 5$, $-6 < \dot{u} < 6$.

$$\frac{dw}{dt} = \varepsilon, \quad \varepsilon \ll 1. \tag{2}$$

This system may be thought of as a strongly non-linear oscillator u driven by a slowly increasing input w. When $\varepsilon = 0$, equation (2) shows that w is a constant. In this limiting case, there are equilibria at $u = \pm \sqrt{w}$ (assuming $w > 0$), and the $u - \dot{u}$ phase plane has a separatrix as shown in Fig. 4. (The parameter m in Fig. 4 is the squared modulus of the elliptic function cn, as in equation (4).) Motions which start inside (outside) the separatrix cannot cross it and so remain inside (outside) it for all time.

For small (positive) ε, equation (2) shows that w grows slowly in time, i.e.

$$w(t) = \varepsilon t + w(0). \tag{3}$$

We may think about this case by imagining a series of "instantaneous phase portraits", each as in Fig. 4 for a constant value of w, strung together in time as if w were increasing quasi-statically. Each such phase portrait will be said to contain "instantaneous integral curves", one of which will be referred to as an "instantaneous separatrix". This notation, while natural and convenient, must be accompanied by a caveat: an instantaneous separatrix is not a true separatrix in the sense that a motion can cross it.

It is just this crossing of the separatrix that we shall be interested in for the purpose of discussing the dynamics of capture vs pass-through. In particular, a motion which starts on an instantaneous integral curve which lies outside the separatrix, may find itself inside the separatrix at some later time. This scenario corresponds to capture, for as we shall show, a motion which so enters the region inside the separatrix will stay there for all time. This process is all the more striking in view of the conservative nature of the problem. In this problem, a captured motion does not asymptotically approach a limiting set, as it does, for example, in the case of a limit cycle which asymptotically attracts everything in its neighborhood. Rather, the region inside the instantaneous separatrix grows larger with time (since w grows larger in time in equation (1)) and the separatrix may be thought of as enveloping motions which would pass too close to it. The fate of a given motion which starts outside the separatrix region is seen as a race between escape to infinity, which will happen in a finite time, and envelopment by the ever growing region inside the separatrix.

We note that no separatrix occurs in equation (1) if w, treated as a constant, is less than zero. Thus we omit consideration of initial conditions $w(0) < 0$ in what follows, since no capture is possible in this case.

We shall approach the system, equations (1) and (2), by using a perturbation theory. This entails perturbing the $\varepsilon = 0$ system, which involves Jacobian elliptic functions [7–9]. We begin by deriving the $\varepsilon = 0$ solution, and then using variation of parameters and averaging to include the effects of a small-ε perturbation.

ELLIPTIC-FUNCTION SOLUTION FOR $\varepsilon = 0$

The general solution to equation (1), in the case that w is a constant, is obtainable by quadrature via conservation of energy. It turns out to have the general form

$$u = \frac{a_1 + a_2 \operatorname{cn}(ct + d, m)}{1 + \operatorname{cn}(ct + d, m)} \tag{4}$$

where $\operatorname{cn}(v, m)$ is the Jacobian elliptic function of argument v and squared modulus m [4, 5]. Here a_1, a_2, c, d and m are constants, only two of which are independent. Instead of obtaining the relationship between a_1, a_2 and c from the conservation of energy, we find it more instructive to proceed directly, as follows. Differentiation of equation (4) gives an expression for the velocity of u:

$$\frac{du}{dt} = c(a_1 - a_2)\frac{\operatorname{sn}\operatorname{dn}}{(1 + \operatorname{cn})^2} \tag{5}$$

where $\operatorname{sn} = \operatorname{sn}(ct + d, m)$, $\operatorname{cn} = \operatorname{cn}(ct + d, m)$, and $\operatorname{dn} = \operatorname{dn}(ct + d, m)$, sn, dn and cn being Jacobian elliptic functions. See Appendix A for some useful identities involving these functions.

Substituting equation (4) and the derivative of equation (5) into the differential equation (1), utilizing some elliptic-function identities, clearing denominators and equating to zero the coefficients of cn^r for $r = 0, 1, 2, 3$ gives three independent equations for a_1, a_2 and c as functions of m. These may be solved to give

$$a_1 = -\frac{c^2}{2}(4m - 5) \tag{6}$$

$$a_2 = -\frac{c^2}{2}(4m + 1) \tag{7}$$

$$c^4 = \frac{4w}{16m^2 - 16m + 1}. \tag{8}$$

Thus the general solution, equations (4) and (5), contains two arbitrary constants, the squared modulus m and the phase d. The squared modulus m determines on which integral curve the motion lies, while the phase d determines where on that curve that motion sits at $t = 0$.

In order for c to be real-valued in equation (8), we must have $c^4 > 0$. But this requires that the sign of $16m^2 - 16m + 1$ be the same as that of w. The roots of $16m^2 - 16m + 1 = 0$ are:

$$m = m_1 = \frac{2 - \sqrt{3}}{4} \simeq 0.06698 \qquad \text{and} \qquad m = m_2 = \frac{2 + \sqrt{3}}{4} \simeq 0.93301. \tag{9}$$

Thus $w > 0$ corresponds to $m < m_1$ and $m > m_2$.

The energy integral associated with equations (1) and (2) for $\varepsilon = 0$ may be written as

$$\frac{\dot{u}^2}{2} - \frac{u^3}{3} + wu = h = \text{constant}. \tag{10}$$

Substituting equations (4) and (5) into equation (10) gives

$$h = h(m) = \frac{-2(2m - 1)(32m^2 - 32m - 1)w^{3/2}}{3(16m^2 - 16m + 1)^{3/2}}. \tag{11}$$

Equations (10) and (11) may be used to plot typical integral curves and the corresponding values of m, see Fig. 4. The separatrix loop corresponds to the value $m = 1$. The closed integral curves lying inside the separatrix correspond to values of m larger than 1, with the equilibrium point lying inside the separatrix loop corresponding to $m \to \infty$. The unbounded integral curves lying outside the separatrix loop and to the left of the separatrix "whiskers" correspond to values of m between m_2 and 1. The integral curves to the right of the separatrix whiskers may be shown to correspond to values of m between $-\infty$ and m_1, with the whiskers corresponding to $m \to -\infty$. (Although the elliptic functions are usually

defined for m between 0 and 1, their values may be extended to all real values of m by using the "reciprocal modulus" and "imaginary modulus" transformations [5].)

The singularity in the denominator of the general solution, equations (4) and (5), namely $1 + \mathrm{cn}(ct + d, m)$, produces an escape to infinity in finite time, provided that $w > 0$ and $m < 1$. (This follows from the fact that $\mathrm{cn}(v, m)$ achieves the value -1 once in each period of duration $4K(m)$, where $K(m)$ is the complete elliptic integral of the first kind.) If, on the contrary, $w > 0$ and $m > 1$, then the cn function takes on values bounded above -1, and the denominator can no longer vanish. This latter case corresponds to motions inside the separatrix, see Fig. 4.

Thus, in the $\varepsilon = 0$ limit in which w, m and d are constants, a typical motion either (i) escapes to infinity, or (ii) remains inside the separatrix. (This statement excludes a set of measure-zero motions which lie on the separatrix or are the equilibria themselves.)

VARIATION OF PARAMETERS

If ε is no longer zero, then w is no longer a constant, but rather varies linearly in t as in equation (3). The parameters m and d, which were constants for $\varepsilon = 0$, now vary in time. Thus a given motion may move from one instantaneous integral curve to another. By examining the behavior of m as a function of time, we will be able to determine on which instantaneous integral curve a motion is located at time t. In particular, we will be interested in when a given motion, which starts on an instantaneous integral curve which lies outside the separatrix (for which $m < 1$), first reaches the separatrix ($m = 1$). Capture will occur if such a motion enters the region inside the separatrix, i.e. achieves $m = 1$, before it escapes to infinity.

We look for a general solution in the case $\varepsilon > 0$ in the form

$$u = u(t, w, m, d) \tag{12}$$

where the functional dependence of u on w, m and d is the same as in the case $\varepsilon = 0$, but now w, m, and d are permitted to vary with time. We find

$$\frac{\mathrm{d}u}{\mathrm{d}t} = \frac{\partial u}{\partial t} + \frac{\partial u}{\partial w}\frac{\mathrm{d}w}{\mathrm{d}t} + \frac{\partial u}{\partial m}\frac{\mathrm{d}m}{\mathrm{d}t} + \frac{\partial u}{\partial d}\frac{\mathrm{d}d}{\mathrm{d}t} \tag{13}$$

and as usual in variation of parameters, we set

$$\frac{\partial u}{\partial w}\frac{\mathrm{d}w}{\mathrm{d}t} + \frac{\partial u}{\partial m}\frac{\mathrm{d}m}{\mathrm{d}t} + \frac{\partial u}{\partial d}\frac{\mathrm{d}d}{\mathrm{d}t} = 0 \tag{14}$$

and obtain

$$\frac{\mathrm{d}^2u}{\mathrm{d}t^2} = \frac{\partial^2 u}{\partial t^2} + \frac{\partial^2 u}{\partial t\,\partial w}\frac{\mathrm{d}w}{\mathrm{d}t} + \frac{\partial^2 u}{\partial t\,\partial m}\frac{\mathrm{d}m}{\mathrm{d}t} + \frac{\partial^2 u}{\partial t\,\partial d}\frac{\mathrm{d}d}{\mathrm{d}t} \tag{15}$$

in which $\dfrac{\partial^2 u}{\partial t^2} = u^2 - w$ where w, m and d are treated as constants, and where $\dfrac{\mathrm{d}^2u}{\mathrm{d}t^2} = u^2 - w(t)$ takes into account the dependence of w, m, and d on time. These terms formally cancel giving

$$\frac{\partial^2 u}{\partial t\,\partial w}\frac{\mathrm{d}w}{\mathrm{d}t} + \frac{\partial^2 u}{\partial t\,\partial m}\frac{\mathrm{d}m}{\mathrm{d}t} + \frac{\partial^2 u}{\partial t\,\partial d}\frac{\mathrm{d}d}{\mathrm{d}t} = 0. \tag{16}$$

This, together with the condition obtained from consideration of the first derivatives, equation (14), gives

$$\frac{\mathrm{d}m}{\mathrm{d}t} = -\frac{\dfrac{\mathrm{d}w}{\mathrm{d}t}\dfrac{\partial u}{\partial w}\dfrac{\partial^2 u}{\partial t\,\partial d} - \dfrac{\partial u}{\partial d}\dfrac{\partial^2 u}{\partial t\,\partial w}}{\dfrac{\partial u}{\partial m}\dfrac{\partial^2 u}{\partial t\,\partial d} - \dfrac{\partial u}{\partial d}\dfrac{\partial^2 u}{\partial t\,\partial m}} \tag{17}$$

and a similar equation for $\dfrac{\mathrm{d}d}{\mathrm{d}t}$ which, however, we shall not require. Substituting the general solution, equations (4) and (5), for u when $\varepsilon = 0$, and using a variety of identities involving

the elliptic functions cn, sn and dn, we obtain the following equation for $m(t)$:

$$\frac{dm}{dt} = \frac{1}{w}\frac{dw}{dt}\frac{16m^2 - 16m + 1}{6}\frac{m(8m-7)\text{cn} - (m-1)(8m-1)}{1+\text{cn}} \tag{18}$$

where $\text{cn} = \text{cn}(ct + d, m)$. This result was obtained by using the computer algebra system MACSYMA [6–9].

We note that equation (18) is exact. We now seek to simplify it by introducing an approximation.

AVERAGING

In order to simplify equation (18), we posit an approximate near-identity transformation valid for small ε, based on the fact that $dw/dt = \varepsilon$, and hence that dm/dt is small. We rewrite equation (18) to emphasize its dependence on cn,

$$\frac{dm}{dt} = \varepsilon\frac{A\,\text{cn} + B}{1+\text{cn}} = \varepsilon g(m, v) \tag{19}$$

where $v = ct + d$ and $\text{cn} = \text{cn}(v, m)$. Then we set

$$m = \bar{m} + \varepsilon f(\bar{m}, v) \tag{20}$$

where f is a function which we may choose at will, and we thus obtain

$$\frac{d\bar{m}}{dt} = \varepsilon\left[g(\bar{m}, v) - \frac{\partial f}{\partial v}\frac{dv}{dt}\right] + O(\varepsilon^2) \tag{21}$$

in which $\dfrac{dv}{dt} = c$. In order to choose f we first compute the indefinite integral of g([5], p. 215), i.e.

$$\int\frac{A\,\text{cn} + B}{1+\text{cn}}\,dv = Bv + (A - B)\left[E(v) - \frac{\text{sn}\,\text{dn}}{1+\text{cn}}\right] \tag{22}$$

in which $E(v)$ is the incomplete elliptic integral of the second kind. A natural choice for f which would eliminate the v-dependence of the right-hand side of equation (21) would be

$$c\frac{\partial f}{\partial v} = g(\bar{m}, v) - \frac{1}{4K}\int_{-2K}^{2K} g(\bar{m}, v)\,dv \tag{23}$$

in which the last term represents the average value of $g(\bar{m}, v)$ along an instantaneous integral curve (for fixed $\bar{m}$) as it reaches from $du/dt = -\infty$ to $+\infty$ in the u–$\dot{u}$ phase plane. This choice is impossible, however, due to the singular behavior of the term $\text{sn}\,\text{dn}/(1 + \text{cn})$ at $v = \pm 2K$ in the indefinite integral of g, equation (22). An alternative choice for f which simplifies equation (21) is

$$c\frac{\partial f}{\partial v} = g(\bar{m}, v) - \frac{1}{2\alpha}\int_{-\alpha}^{\alpha} g(\bar{m}, v)\,dv \tag{24}$$

where $0 < \alpha < 2K$. This avoids the singularity at $\alpha = 2K$, but also excludes from consideration points which lie at the ends of each instantaneous integral curve. Numerical simulation of equations (1) and (2) shows that capture occurs chiefly in the neighborhood of the separatrix, so that excluding the points which lie at the ends of each instantaneous integral curve represents an acceptable compromise.

We choose $\alpha = K$ in the previous equation, since in this case the integral is greatly simplified. This choice will exclude from consideration as candidates for capture those initial conditions which correspond to $K < |v| < 2K$. We refer to the region in the u–$\dot{u}$ plane for which $-K < v < K$ as region $R(t)$. We have displayed the region $R(t)$ in Fig. 5 by noting that at $v = K$, the elliptic functions take on the values $\text{cn} = 0$, $\text{sn} = 1$ and $\text{dn} = \sqrt{1-m}$. From equations (4) and (5), this gives $u = a_1$ and $\dot{u} = c(a_1 - a_2)\sqrt{1-m}$, which, using equations (6)–(9) provides a parametric representation of the boundary curve of region $R(t)$, with m as parameter.

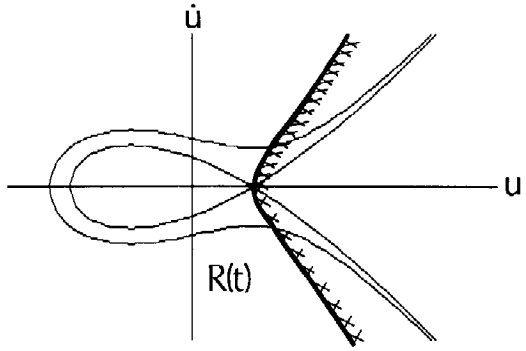

Fig. 5. The region $R(t)$. The flow along an instantaneous integral curve which lies outside the separatrix loop goes from $\dot{u} = -\infty$ to $+\infty$ as v goes from $v = -2K$ to $2K$. The region $R(t)$ is defined by those points along each instantaneous integral curve for which $-K < v < K$. The region $R(t)$ lies to the left of the bold curve. Points on the hatched (right) side of the bold curve will be excluded from consideration as candidates for capture.

Thus we choose f as

$$f = \frac{1}{c}\left[\int_{-K}^{v} g(\bar{m}, v)\,\mathrm{d}v - \frac{v+K}{2K}\int_{-K}^{K} g(\bar{m}, v)\,\mathrm{d}v\right] \tag{25}$$

which evaluates to

$$f = \frac{A-B}{c}\left[E(v) - \frac{vE}{K} - \frac{\mathrm{sn}\,\mathrm{cn}}{1+\mathrm{cn}} + \frac{v\sqrt{1-\bar{m}}}{K}\right] \tag{26}$$

in which K and E are complete elliptic integrals of the first and second kinds, respectively. With this choice of f equation (21) can be cast in the form

$$\frac{\mathrm{d}\bar{m}}{\mathrm{d}t} = \frac{1}{2K}\int_{-K}^{K} \frac{A\,\mathrm{cn} + B}{1+\mathrm{cn}}\,\mathrm{d}v = B + (A-B)\frac{E - \sqrt{1-\bar{m}}}{K} \tag{27}$$

or

$$\frac{\mathrm{d}\bar{m}}{\mathrm{d}t} = \frac{1}{w}\frac{\mathrm{d}w}{\mathrm{d}t}\frac{16\bar{m}^2 - 16\bar{m} + 1}{6} \times\left[(1-\bar{m})(8\bar{m}-1) + (16\bar{m}^2 - 16\bar{m} + 1)\frac{E - \sqrt{1-\bar{m}}}{K}\right]. \tag{28}$$

For brevity of notation in what follows, we shall drop the bar on $\bar{m}$.

ANALYSIS OF THE AVERAGED SYSTEM

The problem of capture may now be stated as follows: for a given initial condition $w(0)$, $m(0)$ and $d(0)$, which of the following two events occurs first:

(i) the ensuing motion escapes from region $R(t)$ (in which case the motion passes through resonance), or

(ii) the slow evolution of m reaches the separatrix value of unity (in which case the motion is captured).

We consider the slow evolution of m first. It will be convenient to write the averaged $\mathrm{d}m/\mathrm{d}t$ equation, equation (28), in the form

$$\frac{\mathrm{d}m}{\mathrm{d}t} = \frac{1}{w}\frac{\mathrm{d}w}{\mathrm{d}t}\mathscr{F}(m) \tag{29}$$

where

$$\mathscr{F}(m) = \frac{16m^2 - 16m + 1}{6}\left[(1-m)(8m-1) + (16m^2 - 16m + 1)\frac{E - \sqrt{1-m}}{K}\right]. \tag{30}$$

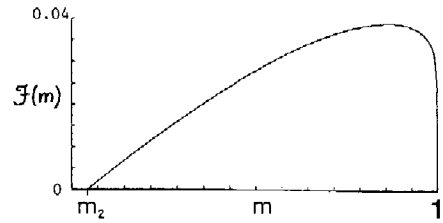

Fig. 6. The function $\mathcal{F}(m)$. See equations (29) and (30).

We present a plot of $\mathcal{F}(m)$ for $m_2 < m < 1$ in Fig. 6. From the observation that $\mathcal{F}(m) > 0$ in this range, it is tempting to conclude that since $dm/dt > 0$, m increases monotonically, eventually evolving to a value of $m > 1$. This would correspond to the motion of a trajectory which enters the region inside the separatrix and becomes captured. However, we may not draw this conclusion because $\mathcal{F}(m) \to 0$ as $m \to 1$, i.e. $m = 1$ is apparently an equilibrium of the m-flow, equation (29). In fact, the averaging approximation breaks down in the neighborhood of $m = 1$, which is indicated by the appearance of K in $\mathcal{F}(m)$, since K and its derivatives with respect to m blow up at $m = 1$.

In order to see what happens to the evolution of m near $m = 1$, we must abandon the averaging model, equation (29), near $m = 1$, and replace it by a "boundary layer" flow obtained directly from the unaveraged m-equation, equation (18). Expanding the right-hand side of equation (18) in a Taylor series about $m = 1$, we obtain

$$\frac{dm}{dt} = \frac{1}{w}\frac{dw}{dt}\frac{1}{6(1+\cosh v)} + O(1-m) \tag{31}$$

where we have used the fact that ([5], p. 25)

$$\mathrm{cn}(v,m) = \operatorname{sech} v + O(1-m). \tag{32}$$

Since the right-hand side of equation (31) is strictly positive in the neighborhood of $m = 1$, we may conclude that m does indeed increase through the value $m = 1$. In order to simplify things, we will take m to depend on w instead of t, which is permissible since w is monotonically increasing with t, cf. equation (3). Then the evolution of m is given by

$$\frac{dm}{dw} = \frac{1}{w}\mathcal{F}(m), \qquad m_2 < m < 1 \tag{33}$$

$$\frac{dm}{dw} = \frac{1}{w}\frac{1}{6(1+\cosh v)} + O(1-m), \qquad m \approx 1. \tag{34}$$

Figure 7 shows the corresponding flow in the w–m plane.

With the foregoing technical difficulty near $m = 1$ taken care of, we might now be tempted to conclude that *all* motions enter the region inside the separatrix ($m > 1$) and become captured. To see that this is not the case, however, we next consider the question of escape from the region $R(t)$. In what follows, "escape" will be used synonymously with "pass-through" to refer to motions which are not captured.

CONDITION FOR ESCAPE

Since for small ε, the quantities w, m and d evolve slowly compared to the time for escape from $R(t)$, we may treat w, m and d as constants for the purpose of discussion of escape times. For fixed w, m and d, the motion proceeds along an instantaneous integral curve in the u–$\dot{u}$ plane, Fig. 4, until the argument $v = ct + d$ of the cn function in u becomes $v = K$, at which point the motion leaves the region $R(t)$. Although the actual time for escape depends in a complicated way on the initial position along the instantaneous integral curve, we may obtain a bound on the escape time from $v_{\text{escape}} < 2K$, i.e. the change in v from one end of the instantaneous integral curve, $v = -K$, to the other, $v = +K$. Therefore, the time for

escape, t_{escape}, is bounded by t^*, where

$$t_{\text{escape}} < t^* = \frac{2K}{c}. \tag{35}$$

In this expression, c and K depend on m and w (assumed fixed). In terms of w, this bound becomes

$$w_{\text{escape}} < w^* = \varepsilon t^* + w(0). \tag{36}$$

Substituting equation (8) for c into equation (36), we obtain

$$w^* = \varepsilon \frac{\sqrt{2}K(m)(16m^2 - 16m + 1)^{1/4}}{w(0)^{1/4}} + w(0) \tag{37}$$

in which the appearance of w in the expression for c is replaced by $w(0)$, valid to $O(\varepsilon^2)$. This may be written in the form

$$w^* = \varepsilon \frac{f(m)}{w(0)^{1/4}} + w(0) \tag{38}$$

where

$$f(m) = \sqrt{2}K(m)(16m^2 - 16m + 1)^{1/4}. \tag{39}$$

For $m \in (m_2, 1)$, $f(m)$ is monotone increasing, with $f(m_2) = 0$ and $f(1) = \infty$.

In order to see which initial conditions lead to motions which escape, Fig. 8 shows w^* plotted as a function of m in the w–m plane, superimposed on the flow lines of Fig. 7 (now shown dotted), for fixed values of ε and $w(0)$. Note that those trajectories which intersect the w^* curve escape, while those trajectories which reach the separatrix $m = 1$ and get captured do not intersect the w^*-curve. The critical trajectory which separates the two cases corresponds to that trajectory which is tangential to the w^*-curve, shown as a solid curve in Fig. 8. (Of course this procedure yields a bound on the initial conditions for capture since w^* represents a bound on w_{escape}.)

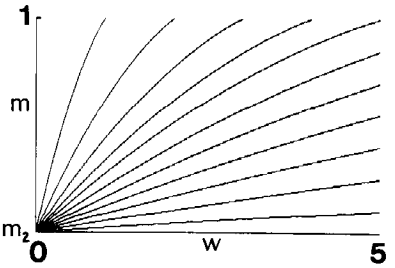

Fig. 7. Flow in the w–m plane for $m > m_2$. All trajectories pass-through $m = 1$. See equations (33) and (34).

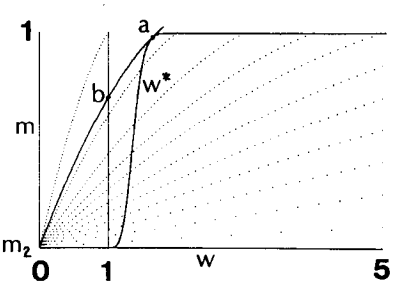

Fig. 8. Plot of w^* of equation (38) as a function of m in the w–m plane for $\varepsilon = 0.1$ and $w(0) = 1$. Also shown (dotted) are the flow lines of Fig. 7. Trajectories which intersect the w^*-curve escape, while trajectories which reach the separatrix $m = 1$ and get captured do not intersect the w^*-curve. The critical trajectory which separates the two cases corresponds to that trajectory which is tangential to the w^*-curve, shown as a solid curve. The point of tangency between the critical trajectory and the w^*-curve is denoted by the letter $a = (w^*, m^*)$. The intersection of the critical trajectory with the curve $w = w(0) = 1$ is denoted by the letter $b = (w(0), m(0))$ and represents an initial condition on a boundary curve in the initial-condition space which separates motions which are captured from those which escape.

The condition for the critical trajectory is that the slope of the w^*-curve, equation (38), equal the slope dw/dm obtained from equation (29) as

$$\frac{dw}{dm} = \frac{\dfrac{dw}{dt}}{\dfrac{dm}{dt}} = \frac{6w}{(16m^2 - 16m + 1)[(1-m)(8m-1) + (16m^2 - 16m + 1)(E - \sqrt{1-m})/K]}. \tag{40}$$

The slope of the w^*-curve is obtained by using the result ([5], p. 282)

$$\frac{dK}{dm} = \frac{E - (1-m)K}{2m(1-m)} \tag{41}$$

and is found from equation (38) to be

$$\frac{dw^*}{dm} = \frac{\varepsilon}{\sqrt{2}\,w(0)^{1/4}} \frac{(m-1)(8m-1)K - (16m^2 - 16m + 1)E}{m(m-1)(16m^2 - 16m + 1)^{1/4}}. \tag{42}$$

Equating the two expressions for the slope, we obtain the following condition for the critical trajectory:

$$\frac{\varepsilon}{w(0)^{5/4}} = \mathcal{G}(m) \tag{43}$$

where

$$\mathcal{G}(m) = \frac{6\sqrt{2}\,Km(1-m)}{[p^2 + pq\sqrt{1-m} + 12m(m-1)K^2]q^{1/4}} \tag{44}$$

$$q = 16m^2 - 16m + 1 \tag{45}$$

$$p = (m-1)(8m-1)K - (16m^2 - 16m + 1)E. \tag{46}$$

We present a plot of $\mathcal{G}(m)$ in Fig. 9. Note it has a discontinuity at $m = m_3 \simeq 0.99423$. For given values of $w(0)$ and ε, the critical trajectory passes through the point (w^*, m^*), where $m^* > m_3$ is defined by $\mathcal{G}(m^*) = \varepsilon/w(0)^{5/4}$, see Fig. 9.

For given values of $w(0)$ and ε, the initial condition corresponding to the critical trajectory is obtained by letting the $m(t)$ slow flow, equation (29), evolve backwards in time, starting from (w^*, m^*), until w reaches $w(0)$. Then the corresponding value of $m(0)$ will generate the critical trajectory. Since equation (29) is intractable, this step must be accomplished by numerical integration.

Once $m(0)$ is known, the instantaneous integral curve corresponding to $m(0)$ and $w(0)$ can be plotted on the u–$\dot{u}$ phase plane using equations (10) and (11), see Fig. 10. This gives a bound on those initial conditions which lead to capture, since any initial conditions outside of the plotted curve, but inside region $R(t)$, are predicted to escape.

A slightly better bound can be obtained by noting that motions which have their initial condition in the upper half-plane, $\dot{u}(0) > 0$, start out more than half-way through the journey along the instantaneous integral curve from $v = -K$ to $+K$. Thus for such motions,

$$t_{\text{escape}} < \frac{K}{c} \tag{47}$$

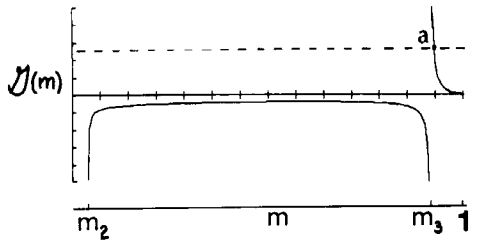

Fig. 9. The function $\mathcal{G}(m)$. The dashed line corresponds to the ordinate $\varepsilon/w(0)^{5/4}$ and its point of intersection with $\mathcal{G}(m)$, denoted by the letter a, corresponds to $m = m^*$. See equations (43) and (44).

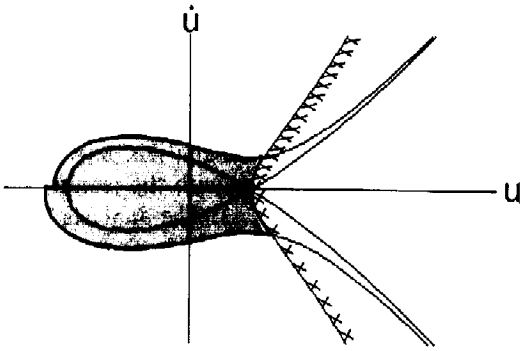

Fig. 10. Approximate region of initial conditions in the u–$\dot{u}$ plane which lead to capture for $\varepsilon = 0.1$ and $w(0) = 1$. The upper and lower boundaries are integral curves which, respectively, correspond to $m = 0.9848492$ and $m = 0.977672$. Substitution of these values of m and the initial value of w ($= 1$) into equations (10) and (11) yields explicit expressions for the upper and lower boundaries of the shaded region. Motions originating in the region $R(t)$ (which lies to the left of the hatched curve, cf. Fig. 5), but outside the shaded region, are predicted to escape capture. Motions originating inside the shaded region, however, may or may not be captured. Region displayed is $-3 < u < 5$, $-6 < \dot{u} < 6$.

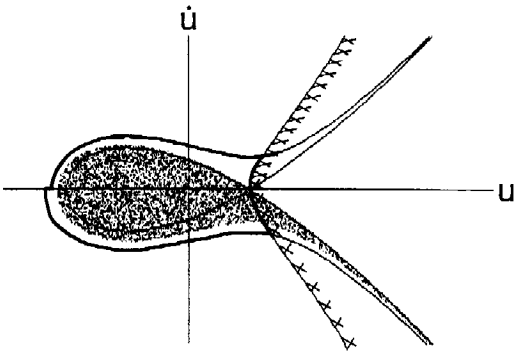

Fig. 11. Results of numerical integration of equation (1) for $\varepsilon = 0.1$ and $w(0) = 1$. Each dot represents an initial condition which leads to capture. Results are superimposed on the results of Fig. 10 obtained analytically. Region displayed is $-3 < u < 5$, $-6 < \dot{u} < 6$.

$$w_{\text{escape}} < \varepsilon \frac{f(m)}{2w(0)^{1/4}} + w(0) \tag{48}$$

which, by comparison with equation (38), corresponds to a value of ε half as large as that associated with the bounding curve in the lower half-plane, $\dot{u}(0) < 0$, see Fig. 10.

COMPARISON WITH NUMERICAL INTEGRATION

In order to check these results, we numerically integrated equation (1) with w as in equation (3), and noted which initial conditions led to capture. This necessitated a practical criterion for capture, which we took as, "if after some fixed time, say T, a motion is still in some fixed region of the phase plane, say $|u| < A$, $|\dot{u}| < B$, then it is considered captured". Here T, A and B must be appropriately chosen for the particular parameters ε and $w(0)$ in question. For example, for $\varepsilon = 0.1$ and $w(0) = 1$, the parameters of Fig. 11, we chose $T = 20$, $A = 5$ and $B = 6$. Since this criterion is rather arbitrary, the results are necessarily approximate, see Fig. 11. For motions originating in the region $R(t)$, the numerically obtained capture region lies inside the bounding region derived using elliptic functions and averaging, as expected. Note, however, that the foregoing analysis offers no information about the fate of motions originating outside the region $R(t)$, i.e. to the right of the hatched curve in Fig. 11. Numerical integration shows that some of these points are captured, while others escape.

SUMMARY AND EXTENSIONS

We have presented the analysis of an abstract dynamical system, equations (1) and (2), which exhibits the phenomenon of resonant capture. The system is derived in the Appendix from a simple mechanical system, Fig. 2. We showed that certain initial conditions lead to capture, while others lead to pass-through. The analysis, based on perturbation theory and elliptic functions, was checked by comparison with the results of numerical integration of the differential equations (1) and (2), see Fig. 11. The analysis, which provided a bound on initial conditions leading to capture, was in reasonable agreement with the numerical results.

We mention some possible extensions of the work presented in this paper:

(1) Our analysis did not take into account the slow evolution of the phase d of the unperturbed solution (4), cf. equation (17), which governs the slow evolution of the squared modulus m. If the slow evolution of d was included in the analysis, better agreement with numerical results would probably result.

(2) The analysis presented in this paper and in refs [2, 3] all assume a small imbalance parameter (ε in equations (1) and (2) and e in equations (B.9) and (B.10)). Preliminary numerical investigations have shown us that for larger values of e, the behavior of equations (B.9) and (B.10) may be chaotic. Analysis of the global dynamics of the system in Fig. 2 is yet to be completed.

(3) We have omitted the effects of damping. This leaves open the question as to how the presence of damping influences the size of the region of initial conditions which lead to capture.

REFERENCES

1. R. J. Kinsey, D. L. Mingori and R. H. Rand, Spinup through resonance of rotating unbalanced systems with limited torque, *Proc. AIAA/AAS Astrodyn. Conf.*, AIAA paper No. 90-2966, Part 2, pp. 805–813. Portland, OR (20–22 August 1990).
2. R. K. Yee, Spinup dynamics of a rotating system with limited torque. M.S. thesis, UCLA (1981).
3. J. A. Sanders and F. Verhulst, *Averaging Methods in Non-linear Dynamical Systems*. Springer, New York (1985).
4. M. Abramowitz and I. A. Stegun, *Handbook of Mathematical Functions*. Dover, New York (1965).
5. P. Byrd and M. Friedman, *Handbook of Elliptic Integrals for Engineers and Physicists*. Springer, Berlin (1954).
6. R. H. Rand and D. Armbruster, *Perturbation Methods, Bifurcation Theory and Computer Algebra*. Springer, New York (1987).
7. V. T. Coppola, Averaging of strongly non-linear oscillators using elliptic functions. Ph.D. thesis, Cornell University, Ithaca (1989).
8. V. T. Coppola and R. H. Rand, Averaging using elliptic functions: approximation of limit cycles. *Acta Mech.* **81**, 125–142 (1990).
9. V. T. Coppola and R. H. Rand, Computer algebra, elliptic functions and chaos, *Proc. 1990 ASME Int. Comp. Engng. Conf.*, Vol. 1, pp. 193–200. Amer. Soc. Mech. Engng (1990).

APPENDIX A

The following identities relating the elliptic functions cn, sn, and dn were found useful in this work and are included here for convenience [4, 5]. We write $\mathrm{sn} = \mathrm{sn}\,v = \mathrm{sn}(v, m)$, etc.

$$\mathrm{sn}^2 + \mathrm{cn}^2 = 1, \qquad m\mathrm{sn}^2 + \mathrm{dn}^2 = 1, \qquad \mathrm{dn}^2 - m\mathrm{cn}^2 = 1 - m \tag{A.1}$$

$$\frac{\mathrm{d}}{\mathrm{d}v}\mathrm{sn} = \mathrm{cn}\,\mathrm{dn}, \qquad \frac{\mathrm{d}}{\mathrm{d}v}\mathrm{cn} = -\mathrm{sn}\,\mathrm{dn}, \qquad \frac{\mathrm{d}}{\mathrm{d}v}\mathrm{dn} = -m\,\mathrm{sn}\,\mathrm{cn}. \tag{A.2}$$

APPENDIX B

Consider a mechanical system consisting of an unbalanced rotor attached to an elastic support and driven by a constant torque as in Fig. 2. Neglecting gravity and friction, the kinetic and potential energies for this system are given by

$$KE = \tfrac{1}{2}M_1 x_t^2 + \tfrac{1}{2}I\theta_t^2 + \tfrac{1}{2}M_2[x_t^2 + 2Ex_t\theta_t\cos\theta + E^2\theta_t^2] \tag{B.1}$$

$$PE = \tfrac{1}{2}kx^2 - A\theta \tag{B.2}$$

where

M_1 = mass of the support
M_2 = mass of the unbalanced part of rotor

I = moment of inertia of the balanced part of rotor about the spin axis
E = distance of mass M_2 from the spin axis
k = support spring constant
A = magnitude of the applied torque.

Lagrange's equations for this system become [3, 2]

$$(M_1 + M_2)x_{tt} + M_2E(\theta_{tt}\cos\theta - \theta_t^2\sin\theta) + kx = 0 \tag{B.3}$$

$$(I + M_2E^2)\theta_{tt} + M_2Ex_{tt}\cos\theta = A. \tag{B.4}$$

This system may be non-dimensionalized by setting [2]

$$T = \sqrt{\frac{k}{M_1 + M_2}}\,t \tag{B.5}$$

$$z = x\sqrt{\frac{M_1 + M_2}{I + M_2E^2}} \tag{B.6}$$

$$L = \frac{(M_1 + M_2)A}{k(I + M_2E^2)} \tag{B.7}$$

$$e = \frac{M_2E}{\sqrt{(M_1 + M_2)(I + M_2E^2)}} \tag{B.8}$$

which gives

$$z_{TT} + z + e(\theta_{TT}\cos\theta - \theta_T^2\sin\theta) = 0 \tag{B.9}$$

$$\theta_{TT} + ez_{TT}\cos\theta = L. \tag{B.10}$$

Numerical integration of these equations [2, 3] shows that, as θ_T approaches the resonant frequency of the support oscillator, i.e. unity, either the θ motion is captured, i.e. θ_T ceases to grow in spite of the applied torque A, or θ_T continues to grow and the θ motion passes through the resonance (see Fig. 3).

In order to derive from equations (B.9) and (B.10) the system (1) and (2) that is treated in this paper, we utilize a series of variable transformations. For the reader's convenience, we summarize these transformations next, and then present the details in the following paragraphs. We begin by assuming the torque parameter L is $O(e)$ and neglecting $O(e^2)$ in equations (B.11)–(B.13), then we transform to polar coordinates in the z–z_T plane in equations (B.14)–(B.18). Next the application of a near-identity transformation, equations (B.19)–(B.31), results in reducing the number of differential equations from four to three. Then attention is restricted to near-resonance dynamics in equations (B.32)–(B.38). Finally, the flow in the resonance manifold is scaled in equations (B.39)–(B.44).

We wish to investigate the dynamics of the system (B.9) and (B.10) in the case that $e \ll 1$. In order to perturb off of $z_{TT} + z = 0$ and $\theta_{TT} = 0$, we set

$$L = eK. \tag{B.11}$$

Neglecting terms of $O(e^2)$, the equations of motion may be written as

$$z_{TT} + z = e\theta_T^2\sin\theta + O(e^2) \tag{B.12}$$

$$\theta_{TT} = eK + ez\cos\theta + O(e^2). \tag{B.13}$$

Next we transform to polar coordinates

$$z = r\sin\psi, \qquad z_T = r\cos\psi \tag{B.14}$$

giving the first-order system

$$r_T = e\Omega^2\sin\theta\cos\psi \tag{B.15}$$

$$\psi_T = 1 - \frac{e}{r}\Omega^2\sin\theta\sin\psi \tag{B.16}$$

$$\theta_T = \Omega \tag{B.17}$$

$$\Omega_T = eK + er\cos\theta\sin\psi. \tag{B.18}$$

We proceed with a near-identity transformation from $(r, \psi, \theta, \Omega)$ to $(\bar{r}, \bar{\psi}, \bar{\theta}, \bar{\Omega})$ equivalent to first-order averaging [3]:

$$r = \bar{r} - \frac{e\bar{\Omega}^2}{2(\bar{\Omega} + 1)}\cos(\psi + \theta) \tag{B.19}$$

$$\psi = \bar{\psi} + \frac{e\bar{\Omega}^2}{2\bar{r}(\bar{\Omega} + 1)}\sin(\psi + \theta) \tag{B.20}$$

$$\theta = \bar{\theta} - \frac{e\bar{r}}{2(\bar{\Omega} + 1)^2}\sin(\psi + \theta) \tag{B.21}$$

$$\Omega = \bar{\Omega} - \frac{e\bar{r}}{2(\bar{\Omega} + 1)}\cos(\psi + \theta) \tag{B.22}$$

which gives

$$\bar{r}_T = -\frac{e}{2}\bar{\Omega}^2\sin(\bar{\psi} - \bar{\theta}) \tag{B.23}$$

$$\bar{\Omega}_T = eK + \frac{e\bar{r}}{2}\sin(\bar{\psi} - \bar{\theta}) \tag{B.24}$$

$$\bar{\theta}_T = \bar{\Omega} \tag{B.25}$$

$$\bar{\psi}_T = 1 - \frac{e}{2\bar{r}}\bar{\Omega}^2\cos(\bar{\psi} - \bar{\theta}). \tag{B.26}$$

We note that the trigonometric terms with the argument $\bar{\psi} - \bar{\theta}$ could not be removed due to vanishing denominators in the neighborhood of the *resonance manifold*

$$\bar{\Omega} = 1. \tag{B.27}$$

Following [3], we set

$$\chi = \bar{\theta} - \bar{\psi} \tag{B.28}$$

which gives the three-dimensional system

$$\bar{r}_T = \frac{e}{2}\bar{\Omega}^2\sin\chi \tag{B.29}$$

$$\bar{\Omega}_T = eK - \frac{e\bar{r}}{2}\sin\chi \tag{B.30}$$

$$\chi_T = \bar{\Omega} - 1 + \frac{e}{2\bar{r}}\bar{\Omega}^2\cos\chi. \tag{B.31}$$

In order to investigate the dynamics in the neighborhood of resonance, we restrict attention to the region of state space for which $\bar{\Omega} = 1 + O(e)$. This makes χ_T be $O(e)$, and hence the equations may be written in the form [3]

$$\chi_{TT} + \frac{e\bar{r}}{2}\sin\chi = eK \tag{B.32}$$

$$\bar{r}_T = \frac{e}{2}\sin\chi. \tag{B.33}$$

These equations may be further simplified by setting

$$\rho = \frac{\bar{r}}{2K} \tag{B.34}$$

$$\eta = \sqrt{eK}\,T \tag{B.35}$$

$$\mu = \frac{\sqrt{e}}{4\sqrt{K^3}} \ll 1 \tag{B.36}$$

giving

$$\chi_{\eta\eta} + \rho\sin\chi = 1 \tag{B.37}$$

$$\rho_\eta = \mu\sin\chi. \tag{B.38}$$

For small μ, ρ is nearly a constant. For constant ρ, the nature of the phase portrait of the χ-equation in the χ–χ_η phase plane depends on whether ρ is greater or smaller than unity. As ρ increases through unity, a pair of equilibrium points bifurcate out of $\chi = \pi/2$. One of these equilibria is a center, while the other is a saddle. The saddle is associated with a separatrix which surrounds the center. Motions which start inside the separatrix correspond to capture while motions which stay outside the separatrix correspond to pass-through. In order to investigate the capture process for small μ, we introduce new coordinates which have their origin at $\rho = 1$ and $\chi = \pi/2$, and which are scaled to simplify the resulting equations. We set

$$\chi = \frac{\pi}{2} + \mu^{1/5}u \tag{B.39}$$

$$\rho = 1 + \tfrac{1}{2}\mu^{2/5}w \tag{B.40}$$

$$\tau = \frac{1}{\sqrt{2}}\mu^{1/10}\eta \tag{B.41}$$

which gives to lowest order in μ,

$$u_{\tau\tau} - u^2 = -w \tag{B.42}$$

$$w_\tau = \varepsilon \tag{B.43}$$

$$\varepsilon = \sqrt{8\mu} \ll 1. \tag{B.44}$$

Equations (B.42) and (B.43) are the equations (1) and (2) investigated in this paper. We have replaced τ by t in equations (1) and (2) for convenience.